ACS Chemical Neuroscience

Letter

pubs.acs.org/chemneuro

Selective Gelatinase Inhibitor Neuroprotective Agents Cross the Blood-Brain Barrier

Major Gooyit,[†] Mark A. Suckow,[‡] Valerie A. Schroeder,[‡] William R. Wolter,[‡] Shahriar Mobashery,[†] and Mayland Chang*[,†]

[†]Department of Chemistry and Biochemistry, University of Notre Dame, Notre Dame, Indiana 46556, United States

[‡]Freimann Life Sciences Center and Department of Biological Sciences, University of Notre Dame, Notre Dame, Indiana 46556, United States

Supporting Information

ABSTRACT: SB-3CT, a potent and selective inhibitor of matrix metalloproteinase-2 and -9, has shown efficacy in several animal models of neurological diseases. One of the greatest challenges in the development of therapeutics for neurological diseases is the inability of drugs to cross the blood-brain barrier. A sensitive bioanalytical method based on ultraperformance liquid chromatography with multiple-reaction monitoring detection was developed to measure levels of SB-3CT, its active metabolite, the α-methyl analogue, and its *p*-hydroxy metabolite in plasma and brain. The compounds are rapidly absorbed and are readily distributed to the brain. The pharmacokinetic properties of these gelatinase inhibitors and the efficacy shown by SB-3CT in animal models of stroke, subarachnoid hemorrhage, and spinal cord injury indicate that this class of compounds holds considerable promise in the treatment of diseases of the central nervous system.

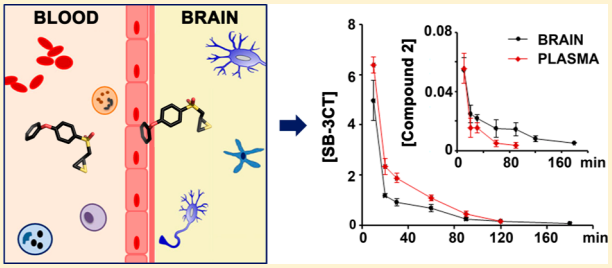

KEYWORDS: *Gelatinase inhibitors, matrix metalloproteinases, brain delivery, SB-3CT*

SB-3CT (compound **1**, Figure 1), is a thiirane-based inhibitor that is selective for matrix metalloproteinase (MMP)-2 and -9,[1] also known as gelatinases. This compound has shown efficacy in a number of neurological diseases, including blocking laminin degradation by MMP-9 and rescuing neurons from apoptosis after transient focal cerebral ischemia,[2] preventing laminin degradation after subarachnoid hemorrhage,[3] reducing cerebral vasopasm caused by subarachnoid hemorrhage,[4] reducing the infiltration of monocytes into the injured spinal cord,[5] and decreasing extravasation and apoptotic cell death after spinal cord injury.[6] The compounds of the thiirane class have a unique mechanism of action, involving ring-opening of the thiirane ring at the active site of gelatinases and generation of the thiolate, which is a picomolar and tight-binding inhibitor.[7]

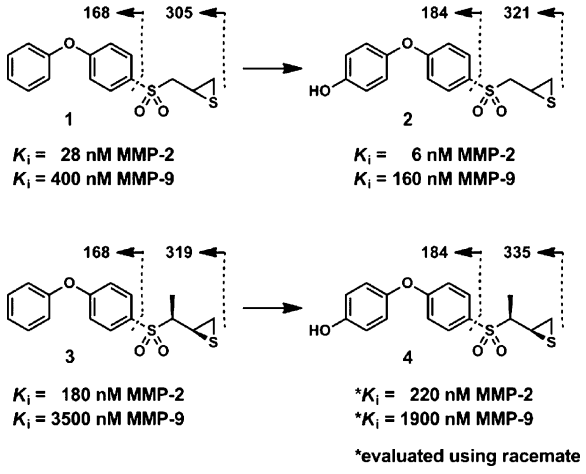

Figure 1. Structures, gelatinase inhibition constants, and mass-spectral fragmentation of SB-3CT (**1**), its active metabolite (**2**), α-methyl derivative (**3**), and its *p*-hydroxy metabolite (**4**).

The blood-brain barrier (BBB) forms a physical separation between circulating blood and the brain parenchyma and consists of tight junctions around endothelial cells surrounded by basement membrane. The BBB prevents pathogens and large hydrophilic molecules from entering the brain, while allowing transport of substances needed by the central nervous system (CNS) such as glucose, fatty acids, and vitamins. One of the most challenging issues in the development of therapeutics for neurological diseases is the inability of drugs to cross the BBB. In fact, greater than 98% of small-molecule drugs and 100% of large-molecule therapeutics do not cross the BBB.[8] Only 5% of small-molecule drugs in the Comprehensive Medicinal Chemistry database treat a mere four CNS diseases: depression, schizophrenia, chronic pain, and epilepsy.[9,10] The vast majority of CNS disorders, including debilitating diseases

Received: June 5, 2012
Accepted: July 30, 2012
Published: July 30, 2012

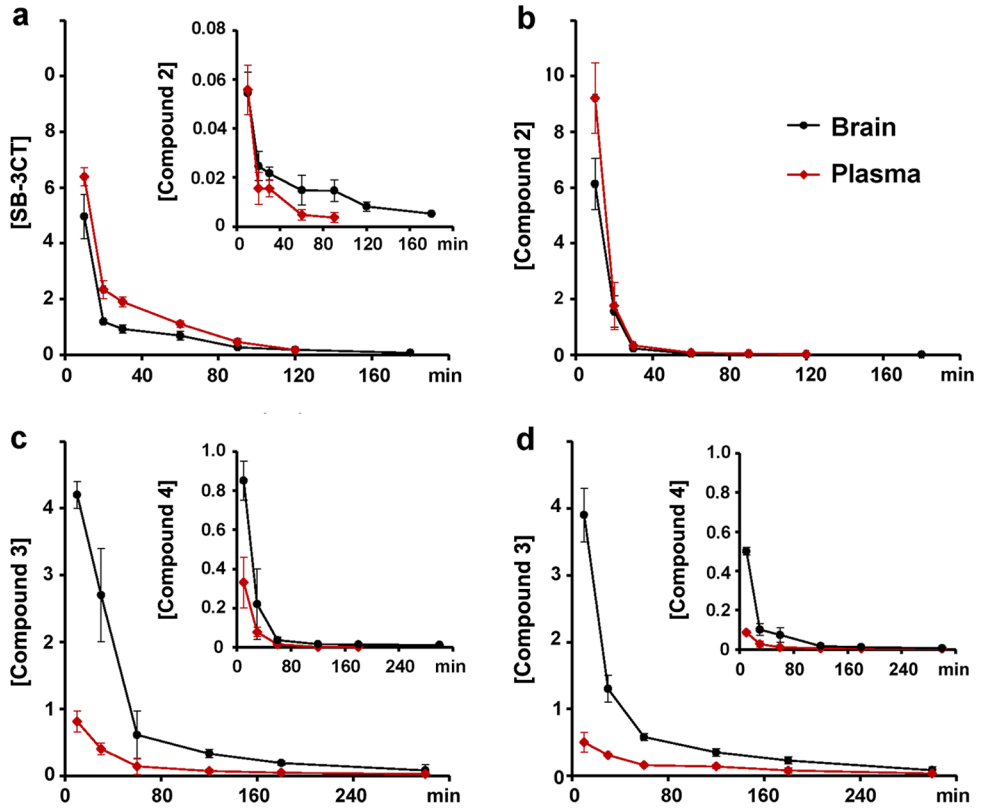

Figure 2. Brain and plasma concentration−time curves of (a) SB-3CT, (b) compound **2**, (c) compound **3** after a single i.p. dose administration at 25 mg/kg to female mice, and (d) compound **3** after a single i.p. dose administration at 25 mg/kg to male mice. Concentrations in pmol/mg tissue for brain and in μM for plasma.

such as stroke, traumatic brain injury (TBI), and spinal cord injury, lack effective drug therapies due in large part to the inability of the molecules to cross the BBB. While strategies to deliver drugs to the brain,[11] including transcranial and transnasal delivery, disruption of the BBB, lipidization, endogenous BBB transporters, and P-glycoprotein inhibitors, have been devised, development of therapeutics that can cross the BBB remains one of the greatest challenges in CNS-drug development.

In the present report, we determined the brain penetration of SB-3CT. Since SB-3CT is primarily metabolized by oxidation of the terminal phenyl ring to a more potent gelatinase inhibitor than the parent compound (compound **2**, Figure 1),[12] we also investigated whether the active metabolite crosses the BBB. Furthermore, we blocked metabolism at the methylene α to the sulfonyl by methylation and evaluated the ability of this analogue (compound **3**) and its metabolite (compound **4**) to cross the BBB.

We first developed a bioanalytical method for determination of levels of compounds **1**−**4** in plasma and brain. SB-3CT has a poor UV chromophore and is poorly ionizable, posing a technical challenge. We were finally able to develop a sensitive method based on ultraperformance liquid chromatography (UPLC) using electrospray ionization (ESI) in the negative mode with multiple-reaction monitoring (MRM) for the transition 305 → 168 m/z. The method was linear up to 30 μM, with coefficients of determination, R^2, of 0.999; the limit of quantification was 0.02 μM. Similar methods for the transitions 321 → 184 m/z, 319 → 168 m/z, and 335 → 184 m/z were developed for compounds **2**, **3**, and **4**, respectively. The limits of quantification for compounds **2**, **3**, and **4** were 0.005, 0.02, and 0.004 μM, respectively. The interday accuracy and precision of the assay were evaluated over 3 days at two quality control (QC) levels (low and high) for brain samples and at three QC levels (low, medium, and high) for plasma samples (see Tables S1 and S2 in the Supporting Information). The deviation values were within the acceptable criteria of ±20% at low QC levels and ±15% at medium and high QC levels. The extraction efficiency of SB-3CT and compounds **2**−**4** was also determined at two QC levels for brain samples and at three QC levels for plasma samples. The absolute recoveries from brain samples ranged from 89.1% to 107%, while those from plasma samples were from 94.4% to 116% (Table S3 in the Supporting Information).

We then administered a single dose of SB-3CT or compounds **2** or **3** intraperitoneally (i.p.) to female mice at 25 mg/kg. This is the same dose level and the same route of administration given in the transient focal cerebral ischemia study. Levels of SB-3CT in plasma of 6.4 ± 0.3 μM were maximal at 10 min, the first time point collected, decreasing to 0.17 ± 0.04 μM at 120 min, and nonquantifiable thereafter (Figure 2a and Table S4 in the Supporting Information). Levels of SB-3CT were slightly lower in brain than in plasma, 5.0 ± 0.8 pmol/mg (equivalent to 5.0 ± 0.8 μM, assuming a density of 1 g/mL) at 10 min and 0.067 ± 0.043 pmol/mg at 180 min. Brain levels of SB-3CT remained above the K_i for MMP-9 of 400 nM for 60 min. However, SB-3CT binds to MMP-9 as a thiolate that is generated at the active site with a K_i value of 2.1 nM, indicating that systemic levels of SB-3CT were well above the K_i of the thiolate for >180 min. Systemic exposure, as measured by $AUC_{0-\infty}$, was 179 μM·min in plasma and 122 pmol·min/mg in brain (Table 1); the brain to plasma AUC

dx.doi.org/10.1021/cn300062w | ACS Chem. Neurosci. 2012, 3, 730−736

Table 1. Pharmacokinetic Parameters of SB-3CT and Compound 2 after a Single i.p. Dose to Female Mice

	SB-3CT after dose of SB-3CT		compound **2** after dose of SB-3CT		compound **2** after dose of compound **2**	
parameter	brain	plasma	brain	plasma	brain	plasma
AUC_{0-last}[a]	118	174	2.61	1.25	82.8	120
$AUC_{0-\infty}$[a]	122	179	3.31	1.65	82.8	121
$t_{1/2\alpha}$ (min)	4.8	6.9	8.8	5.4	4.2	4.2
$t_{1/2\beta}$ (min)	46	22	94	78	29	31
$brain_{AUC}$/$plasma_{AUC}$	0.68		2.0		0.68	

[a]AUC in pmol·min/mg for brain and in μM·min for plasma.

ratio was 0.68, indicating that SB-3CT crossed the BBB. SB-3CT distributed to the brain rapidly with $t_{1/2\alpha}$ of 4.8 min and an elimination half-life of 46 min.

Levels of compound **2** after a single 25 mg/kg i.p. dose of SB-3CT were significantly lower than those of SB-3CT. Maximal levels of compound **2** of 0.056 ± 0.010 μM in plasma and 0.054 ± 0.009 pmol/mg in brain were achieved at 10 min (Figure 2a inset and Table S4 in the Supporting Information). Levels of compound **2** were not quantifiable in plasma at 120 min and were 0.0052 ± 0.0003 in brain at 180 min. $AUC_{0-\infty}$ was 1.65 μM·min in plasma and 3.31 pmol·min/mg in brain; the ratio of brain to plasma $AUC_{0-\infty}$ was 2.0 (Table 1). As with the parent SB-3CT, its metabolite (compound **2**) crossed the BBB. Brain $AUC_{0-\infty}$ for SB-3CT was 37-fold higher than that for compound **2**. Levels of compound **2** in brain were below the K_i for MMP-9 of 160 nM, indicating that the efficacy seen in animal models is likely due to the parent SB-3CT.

Subsequently, we administered to female mice a single 25 mg/kg i.p. dose of compound **2**. Maximal levels of compound **2** of 9.2 ± 1.3 μM in plasma and 6.1 ± 0.9 pmol/mg in brain were observed at 10 min (Figure 2b and Table S4 in the Supporting Information). At 180 min, levels were nonquantifiable in plasma and were 0.0018 ± 0.0032 pmol/mg in brain. $AUC_{0-\infty}$ was 121 μM·min in plasma and 82.8 pmol·min/mg in brain (Table 1). The ratio of brain to plasma AUC was 0.68, indicating that compound **2** crossed the BBB. Like SB-3CT, compound **2** distributed to the brain rapidly with $t_{1/2\alpha}$ of 4.2 min and an elimination half-life of 29 min. However, compound **2** has a residence time of 24.5 min, which together with the pharmacokinetic (PK) half-life prolongs enzyme occupancy and pharmacological action.

We next investigated the regional brain distribution of SB-3CT and compound **2**. Different brain regions including brain stem, cerebellum, cortex, hippocampus, and striatum were dissected from whole brains at 10 min after i.p. administration of SB-3CT and compound **2** to female mice at 25 mg/kg. As shown in Table 2, SB-3CT and compound **2** distributed to all regions of the brain, with brain region to plasma concentration ratios ranging from 0.48 to 1.1.

Another major metabolic pathway of SB-3CT involves oxidation at the α-position to the sulfonyl moiety and generation of the corresponding sulfinic acid. We had previously shown that incorporation of a methyl substituent at the α-position to the sulfonyl group blocked oxidation at that position and also increased metabolic stability.[13] Although the α-methyl derivative **3** is less potent against the gelatinases (9-fold less active against MMP-9) than SB-3CT, its increased metabolic stability might have the advantage of sustained higher brain and blood levels when administered in vivo. To ascertain this, we investigated the PK disposition of compound **3** following a single i.p. dose to female mice at 25 mg/kg. Maximal levels of compound **3** were observed at 10 min, with preferential distribution to the brain (4.2 ± 0.2 pmol/mg) compared to 0.81 ± 0.16 μM in plasma (Figure 2c and Table S5 in the Supporting Information). Levels of **3** were quantifiable up to 300 min with concentrations of 0.079 ± 0.088 pmol/mg in brain and 0.023 ± 0.027 μM in plasma. Results showed that **3** crossed the BBB, with brain to plasma $AUC_{0-\infty}$ ratio of 5.0. Systemic exposure of **3** of 41.8 μM·min in plasma was 4-fold lower than that of SB-3CT. However, brain $AUC_{0-\infty}$ of **3** of 211 pmol·min/mg was 1.7-fold higher compared to SB-3CT. Furthermore, the elimination half-lives of **3** were significantly longer (96 min in brain and 114 min in plasma) compared to those of SB-3CT. These observations could be attributed to the fact that compound **3** does not experience metabolism at the α-position to the sulfonyl group, in contrast to SB-3CT, and thereby resulting in sustained systemic levels and prolonged half-lives.

As with SB-3CT, compound **3** is metabolized by hydroxylation at the *para*-position of the terminal phenyl ring to give compound **4**. Levels of metabolite **4** were considerably lower compared to the parent **3**, with maximal levels of 0.85 ± 0.10 pmol/mg in brain and 0.33 ± 0.13 μM in plasma observed at 10 min after i.p. administration of **3** (Figure 2c inset and Table S5 in the Supporting Information). Brain $AUC_{0-\infty}$ of **4** was 6-fold lower than that for the parent **3**. Compound **4** also distributed extensively into the brain with a systemic exposure of 32.2 pmol·min/mg, which was 4-fold higher than that in plasma (8.13 μM·min). Compound **4**, generated from **3**, had a long elimination half-life of 559 min in the brain. However, levels of compound **4** in brain were below the K_i for MMP-9 of 1.9 μM.

Table 2. Regional Brain Distribution of SB-3CT and Compound 2[a]

	SB-3CT after dose of SB-3CT		compound **2** after dose of SB-3CT		compound **2** after dose of compound **2**	
	conc[b]	ratio[c]	conc[b]	ratio[c]	conc[b]	ratio[c]
whole brain	5.0 ± 0.8	0.78 ± 0.13	0.054 ± 0.009	0.96 ± 0.23	6.1 ± 0.9	0.66 ± 0.14
brain stem	4.2 ± 0.8	0.66 ± 0.13	0.059 ± 0.004	1.1 ± 0.2	5.8 ± 0.6	0.63 ± 0.11
cerebellum	3.1 ± 0.5	0.48 ± 0.08	0.050 ± 0.008	0.89 ± 0.17	4.9 ± 0.6	0.53 ± 0.10
cortex	3.6 ± 0.6	0.56 ± 0.10	0.061 ± 0.027	1.1 ± 0.5	4.9 ± 0.7	0.53 ± 0.11
hippocampus	3.9 ± 0.6	0.61 ± 0.10	0.035 ± 0.003	0.63 ± 0.12	5.4 ± 0.5	0.59 ± 0.10
striatum	4.6 ± 0.3	0.72 ± 0.06	0.045 ± 0.008	0.80 ± 0.20	5.6 ± 0.8	0.61 ± 0.12
plasma	6.4 ± 0.3		0.056 ± 0.010		9.2 ± 1.3	

[a]Regional brain distribution determined at 10 min after i.p. dose of SB-3CT or compound **2** to female mice; 9 mice were dosed and brain regions pooled from 3 mice. [b]Concentrations in pmol/mg tissue for brain and in μM for plasma. [c]Ratio of the concentration in brain region to plasma.

dx.doi.org/10.1021/cn300062w | ACS Chem. Neurosci. 2012, 3, 730−736

Gender differences in metabolism and PK are contributing factors to individual differences in drug efficacy and toxicity. To determine whether there would be significant differences of PK profiles in female and male mice, we initially incubated SB-3CT and compounds **2** and **3** in both female and male mouse liver S9. The half-lives of all three compounds were similar in both genders. SB-3CT had a half-life of 3.3 ± 0.1 and 3.1 ± 0.3 min in female and male mouse liver S9, respectively. Compound **2** had a slightly longer half-life of 9.2 ± 0.3 min in female mouse liver S9 compared to 8.2 ± 0.2 min in male mouse. Compound **3** had comparable half-lives in both sexes (5.5 ± 0.6 and 5.4 ± 0.5 min in female and male mouse liver S9, respectively). To further shed light on gender differences in drug metabolism and PK, we administered compound **3** to male mice at 25 mg/kg, the same dose level previously given to the female littermates. The concentration−time curves and PK properties of **3**, and metabolite **4**, after i.p. administration of **3** to male mice are shown in Figure 2d and Table S5 (Supporting Information). Similar to SB-3CT and **2**, compound **3** preferentially distributed to the brain in male mice, with brain to plasma $AUC_{0-\infty}$ ratio of 4.1. Maximal brain levels of **3** of 3.9 ± 0.4 pmol/mg were observed at 10 min and were comparable to those in female mice (4.2 ± 0.2 pmol/mg). Brain $AUC_{0-\infty}$ of **3** of 174 pmol·min/mg in male mice was slightly lower than that in female mice; however, there were no significant gender differences in plasma systemic exposures of **3**. The brain elimination half-life of **3** of 87 min in male mice was slightly shorter than that observed in the female littermates.

As observed in female mice, the levels of compound **4** after i.p. administration of **3** to male mice were lower than those of the parent **3** (Figure 2d inset and Table S5 in the Supporting Information). Compound **4** also distributed preferentially to the brain, with a brain to plasma $AUC_{0-\infty}$ ratio of 3.6. In general, levels of compound **4**, generated after administration of **3** to male mice, were lower than those observed in female mice. Brain and plasma $AUC_{0-\infty}$ of **4** were approximately 2-fold lower in males compared to those in female mice, suggesting that higher glucuronidation and sulfation activity in males than females. Slower metabolism of acetaminophen via less glucuronidation and sulfation has been observed in female mice than in males.[14] The brain elimination half-life of 110 min of **4** in male mice was considerably shorter than that in female mice, while the plasma elimination half-life of **4** is 1.5-fold longer in male mice than in female mice.

Brain levels of compound **3** were above the K_i for MMP-9 for 10 min, while those of the metabolite **4** were below the K_i for MMP-9. However, the brain concentrations of compound **3** remained above the K_i of 180 nM for MMP-2 for 180 min while compound **4** had brain levels above the K_i of 220 nM for MMP-2 for at least 10 min. In addition, the residence time of compound **3** for MMP-2 was 1.5-fold longer than that for MMP-9. These data suggested that compound **3** might find use in the treatment of MMP-2-dependent neurological diseases.

Gelatinases, in particular MMP-9, are important targets of inhibition in the treatment of various neurological diseases. SB-3CT, compounds **2** and **3** are potent and selective inhibitors of gelatinases (MMP-2 and MMP-9). These compounds are rapidly absorbed and distributed to the brain. They also do not accumulate in the brain and are eliminated (data not shown from multiple dose studies). The clearance of this class of compounds from the brain suggests that these compounds would not cause unwanted neurotoxic effects. In fact, SB-3CT-treatment for 7 days in a permanent mouse model of ischemia is neuroprotective.[15] NXY-059, a free radical trapping agent that failed in clinical trials for acute ischemic stroke, has been reported to lack BBB penetration.[16] Recently, NXY-059 was shown to have limited brain penetration with maximal brain concentrations of 6 pmol/mg (equivalent to approximately 1% of plasma concentration) after continuous intravenous infusion to rats at 125 mg/kg.[17] However, NXY-059 was able to form radical adducts and prevent salicylate oxidation with IC_{50} of 298 μM,[18] a concentration that is not likely to be achieved given the poor brain penetration ability of the compound. Statins are inhibitors of 3-hydroxy-3-methylglutaryl coenzyme A (HMGCoA) reductase that have shown efficacy in animal models of TBI, exerting anti-inflammatory effects, reducing cerebral edema, and decreasing BBB damage.[19−21] Rosuvastatin in a small clinical trial in patients with moderate TBI improved amnesia; however, it showed no differences in 3-month outcomes.[22] This may be due to the inability of the hydrophilic rosuvastatin to enter the brain.[23] Progesterone has shown neuroprotective effects in animal models of spinal cord injury, stroke and TBI,[24−26] and has shown possible signs of benefit in clinical trials in patients after TBI.[27] Interestingly, progesterone decreases BBB damage after permanent focal ischemia by reducing MMP-2 and MMP-9 activity.[28] The desirable PK properties of the thiirane class of gelatinase inhibitors and the efficacy shown by SB-3CT in animal models of stroke, subarachnoid hemorrhage, and spinal cord injury makes this class of compounds promising in the treatment of CNS diseases.

METHODS

Syntheses and Formulation of SB-3CT, Compounds 2−4, and Internal Standard. SB-3CT, compounds **2**−**4**, and the internal standard **5** were synthesized as described previously.[1,29] SB-3CT was formulated as a solution at a concentration of 10 mg/mL in 25% DMSO/65% PEG-200/10% water. Compound **2** was dissolved in 70% propylene glycol/30%water at a concentration of 10 mg/mL. Compound **3** was prepared at concentrations of 10 and 12.5 mg/mL in 25% DMSO/65% PEG-200/10% water. The dosing solutions were sterilized by filtration through an Acrodisc syringe filter (Pall Life Sciences, Ann Arbor, MI, 0.2 μm, 13 mm diameter, PTFE membrane).

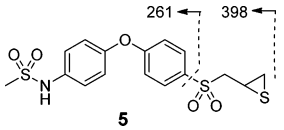

5

Gelatinase Inhibition. The thiolate of SB-3CT was synthesized as described earlier,[7] The K_i^{app} values of the thiolate were estimated by nonlinear regression using Morrison's equation for analysis of tight-binding inhibition.[30,31] The inhibition constant, K_i, of the thiolate was then calculated by $K_i^{app}/(1 + S/K_m)$, where S is the substrate concentration and K_m is the Michaelis constant.

Animals. Mice (female C57Bl/6J, 6−8-weeks old, 17−20 g body weight, and male C57Bl/6J, 6−8-weeks old, 22−25 g body weight specific pathogen free, $n = 3$ per time point) were obtained from The Jackson Laboratory (Bar Harbor, ME). All procedures were performed in accordance with the University of Notre Dame Institutional Animal Care and Use Committee. Mice were provided with Teklad 2019 Extruded Rodent Diet (Harlan, Madison, WI) and water ad libitum. Animals were

dx.doi.org/10.1021/cn300062w | ACS Chem. Neurosci. 2012, 3, 730−736

maintained in polycarbonate shoebox cages with hardwood bedding in a room under a 12:12 h light/dark cycle and at 72 ± 2 °F.

Animal Dosing and Sample Collection. Mice (n = 3 per time point per compound) were administered a single intraperitoneal (i.p.) 50 μL dose of SB-3CT, compound **2** or compound **3** at 25 mg/kg. Mice were anesthetized with an i.p. injection of rodent cocktail (ketamine/xylazine/acepromazine diluted with sterile saline). Terminal blood samples were collected in heparin through the posterior vena cava at 10, 20, 30, 60, 90, 120, 180, and 300 min. Whole brain samples were harvested after transcardiac perfusion with saline, weighed, and immediately flash frozen in liquid nitrogen and stored at −80 °C until analysis. Blood samples were stored on ice and centrifuged to collect plasma. For regional brain distribution, an additional 9 mice were given a single dose i.p. injection of SB-3CT or compound **2** at 25 mg/kg and sacrificed at 10 min. Whole brain samples were collected as described earlier, rapidly dissected into different regions (cortex, striatum, hippocampus, cerebellum, and brain stem), weighed, and immediately frozen in dry ice. Brain regions were pooled from 3 mice.

Sample Analysis. A 75 μL aliquot of plasma was mixed with 150 μL of internal standard in acetonitrile to a final concentration of 1.25 μM. The sample was centrifuged at 10 000g for 10 min. Brain samples were weighed and homogenized for 5 min in one volume equivalent of cold acetonitrile, containing an internal standard, using a bullet blender (Next Advance, Inc., Averill Park, NY). For regional brain distribution, the striatum, hippocampus, cerebellum, and brain stem samples were pooled from 3 different mice for analysis. The homogenates were centrifuged twice at 20 000g for 20 min at 4 °C. The supernatants from plasma and brain samples were collected and analyzed by reversed-phase UPLC/(−)-ESI-MRM of the transitions 305→168 for SB-3CT, 321→184 for compound **2**, 319→168 for compound **3**, 335→184 for compound **4**, and 398→261 for the internal standard. Standard curves of SB-3CT and compounds **2**−**4** were prepared by fortification of blank mouse plasma (and blank brain) with SB-3CT, compound **2**, **3**, or **4** at concentrations up to 30 μM. Quantification was performed using peak area ratios relative to the internal standard and linear regression parameters were calculated from the calibration curve standards prepared in blank mouse plasma (and blank brain).

Quality Control Samples and Extraction Efficiency. Quality control samples were prepared daily for 3 days at two levels (low and high) in brain and at three levels (low, medium, and high) in plasma. The preparation of QC samples was the same as described in the Sample Analysis section. Blank brain and plasma were spiked with standard SB-3CT, compound **2**, **3**, or **4** to produce final concentrations corresponding to low QC of 0.10 pmol/mg in brain for SB-3CT and compound **3** (0.050 pmol/mg for **2** and **4**), or 0.10 μM in plasma for SB-3CT and **3** (0.050 μM for **2** and **4**), medium QC of 2 pmol/mg in brain or 2 μM in plasma, and high QC of 20 pmol/mg in brain or 20 μM in plasma. Standard calibration curves were prepared daily by fortification of blank mouse brain (and blank plasma) with SB-3CT, compound **2**, **3**, or **4** at concentrations up to 30 pmol/mg brain or 30 μM in plasma. Quantification was performed as described above. The extraction efficiency of SB-3CT, compound **2**, **3**, or **4** was evaluated by comparing peak area ratios (relative to the internal standard) of the extracted compounds with the unextracted authentic standards at two QC levels in brain (0.10 and 20 pmol/mg for SB-3CT and compound **3**; 0.050 and 20 μM for **2** and **4**) and at three QC levels in plasma (0.10, 2, and 20 pmol/mg for SB-3CT and compound **3**; 0.050, 2, and 20 μM for **2** and **4**).

Liquid Chromatography/Mass Spectrometry. The chromatographic system consisted of a Waters Acquity UPLC System (Waters Corporation, Milford, MA) equipped with a binary solvent manager, an autosampler, a column heater, and a photodiode array detector. All mass spectrometric experiments were performed with a Waters TQD tandem quadrupole detector (Milford, MA) monitored with MassLynx MS software. Mass spectrometry acquisition was performed in the negative electrospray ionization mode with multiple reaction monitoring. The capillary voltage, cone voltage, extractor voltage, and RF lens voltage were set at 2.8 kV, 35 V, 3 V, and 0.3 V, respectively. Desolvation gas flow rate was 650 L/h (nitrogen), and the cone gas flow rate was 50 L/h (nitrogen). The source temperature and desolvation temperature were held at 150 and 350 °C, respectively. Samples were analyzed on an Acclaim RSLC 120 C18 column (2.2 μm, 2.1 mm i.d. × 100 mm, Dionex, Sunnyvale, CA). The mobile phase consisted of elution at 0.5 mL/min with 85% A/15% B for 1 min, followed by a 6-min linear gradient to 10% A/90% B and then 10% A/90% B for 2 min (A = water; B = acetonitrile).

Pharmacokinetic Parameters. The area under the mean concentration−time curve up to the last quantifiable sampling time ($AUC_{0\text{-last}}$) was calculated by the trapezoidal rule using the pharmacokinetic software PK Solutions (version 2.0, Summit Research Services, Montrose, CO). $AUC_{0\text{-}\infty}$ was calculated as $AUC_{0\text{-last}} + (C_{last}/k)$, where C_{last} is the concentration at the last quantifiable sampling time and k is the elimination rate constant. Half-lives ($t_{1/2\alpha}$ and $t_{1/2\beta}$) were estimated from the linear portion of the initial or terminal linear portion of the concentration−time data by linear regression, where the slope of the line was the rate constant k and $t_{1/2\alpha} = \ln 2/k$.

Stability in Mouse Liver S9. Incubations consisted of mouse pooled male or female S9 (1.0 mg; BD Biosciences, Woburn, MA), NADPH (final concentration 0.5 mM), and 10 μM SB-3CT or compound **2** or **3** in potassium phosphate buffer (100 mM, pH 7.4) at 37 °C in a total volume of 0.5 mL. Aliquots were drawn at different time points, and the reactions were terminated by the addition of one volume of internal standard (final concentration 1 μM) in acetonitrile. The precipitated protein was centrifuged (10 min, 10 000g), and the supernatant was analyzed by reversed phase UPLC/(−)-ESI-MRM as detailed above. The half-lives were calculated using the first order rate law.

■ ASSOCIATED CONTENT

Ⓢ Supporting Information

Tables S1 and S2 showing interday accuracy, precision, and relative error of SB-3CT and compounds **2**−**4** in spiked brain and plasma samples, respectively; Table S3 showing the extraction efficiency from brain and plasma samples; Table S4 reporting the concentrations of SB-3CT and compound **2**, and Table S5 showing the concentrations and PK parameters of compounds **3** and **4** after a single i.p. dose to female and male mice. This material is available free of charge via the Internet at http://pubs.acs.org.

■ AUTHOR INFORMATION

Corresponding Author

*E-mail: mchang@nd.edu.

Present Address

Department of Chemistry and Biochemistry, University of Notre Dame, Notre Dame, IN 46556.

Author Contributions

M.G. synthesized compounds **2**–**4** and performed the experiments. M.G. and M.C. designed the experiments and analyzed the results. M.A.S., V.A.S., and W.R.W. performed the in-life portion of the animal studies. M.G., S.M., and M.C. wrote the manuscript.

Funding

This work was supported by grant CA122417 from the National Institutes of Health. M.G. is a Fellow of the Chemistry-Biochemistry-Biology Interface Program, supported by a training grant GM075762 from the National Institutes of Health.

Notes

The authors declare no competing financial interest.

■ ACKNOWLEDGMENTS

We thank In Taek Lim for synthesis of SB-3CT.

■ REFERENCES

(1) Brown, S., Bernardo, M. M., Li, Z. H., Kotra, L. P., Tanaka, Y., Fridman, R., and Mobashery, S. (2000) Potent and selective mechanism-based inhibition of gelatinases. *J. Am. Chem. Soc. 122* (28), 6799–6800.

(2) Gu, Z., Cui, J., Brown, S., Fridman, R., Mobashery, S., Strongin, A. Y., and Lipton, S. A. (2005) A highly specific inhibitor of matrix metalloproteinase-9 rescues laminin from proteolysis and neurons from apoptosis in transient focal cerebral ischemia. *J. Neurosci. 25* (27), 6401–6408.

(3) Guo, Z., Sun, X., He, Z., Jiang, Y., Zhang, X., and Zhang, J. H. (2010) Matrix metalloproteinase-9 potentiates early brain injury after subarachnoid hemorrhage. *Neurol Res 32* (7), 715–720.

(4) Wang, Z., Fang, Q., Dang, B. Q., Shen, X. M., Shu, Z., Zuo, G., He, W. C., and Chen, G. (2012) Potential contribution of matrix metalloproteinase-9 (mmp-9) to cerebral vasospasm after experimental subarachnoid hemorrhage in rats. *Ann. Clin. Lab. Sci. 42* (1), 14–20.

(5) Zhang, H., Trivedi, A., Lee, J. U., Lohela, M., Lee, S. M., Fandel, T. M., Werb, Z., and Noble-Haeusslein, L. J. (2011) Matrix metalloproteinase-9 and stromal cell-derived factor-1 act synergistically to support migration of blood-borne monocytes into the injured spinal cord. *J. Neurosci. 31* (44), 15894–15903.

(6) Yu, F., Kamada, H., Niizuma, K., Endo, H., and Chan, P. H. (2008) Induction of mmp-9 expression and endothelial injury by oxidative stress after spinal cord injury. *J. Neurotrauma 25* (3), 184–195.

(7) Forbes, C., Shi, Q., Fisher, J. F., Lee, M., Hesek, D., Llarrull, L. I., Toth, M., Gossing, M., Fridman, R., and Mobashery, S. (2009) Active site ring-opening of a thiirane moiety and picomolar inhibition of gelatinases. *Chem. Biol. Drug Des. 74* (6), 527–534.

(8) Pardridge, W. M. (2007) Blood-brain barrier delivery. *Drug Discovery Today 12* (1–2), 54–61.

(9) Ghose, A. K., Viswanadhan, V. N., and Wendoloski, J. J. (1999) A knowledge-based approach in designing combinatorial or medicinal chemistry libraries for drug discovery. 1. A qualitative and quantitative characterization of known drug databases. *J. Comb. Chem. 1* (1), 55–68.

(10) Lipinski, C. A. (2000) Drug-like properties and the causes of poor solubility and poor permeability. *J. Pharmacol. Toxicol. Methods 44* (1), 235–249.

(11) Pardridge, W. M. (2005) The blood-brain barrier: bottleneck in brain drug development. *NeuroRx 2* (1), 3–14.

(12) Lee, M., Villegas-Estrada, A., Celenza, G., Boggess, B., Toth, M., Kreitinger, G., Forbes, C., Fridman, R., Mobashery, S., and Chang, M. (2007) Metabolism of a highly selective gelatinase inhibitor generates active metabolite. *Chem. Biol. Drug Des. 70* (5), 371–382.

(13) Gooyit, M., Lee, M., Hesek, D., Boggess, B., Oliver, A. G., Fridman, R., Mobashery, S., and Chang, M. (2009) Synthesis, kinetic characterization and metabolism of diastereomeric 2-(1-(4-phenoxyphenylsulfonyl)ethyl)thiiranes as potent gelatinase and MT1-MMP inhibitors. *Chem. Biol. Drug Des. 74* (6), 535–546.

(14) Dai, G., He, L., Chou, N., and Wan, Y. J. (2006) Acetaminophen metabolism does not contribute to gender difference in its hepatotoxicity in mouse. *Toxicol. Sci. 92* (1), 33–41.

(15) Cui, J.; Chen, S.; Zhang, C.; Meng, F.; Wu, W.; Hu, R.; Hadass, O.; Lehmidi, T.; Blair, G. J.; Lee, M.; Chang, M.; Mobashery, S.; Sun, G. Y.; Gu, Z. (2012) Inhibition of MMP-9 by a selective gelatinase inhibitor protects neurovasculature from embolic focal cerebral ischemia. *Mol. Neurodegener. 7* (21), DOI:10.1186/1750-1326-7-21.

(16) Savitz, S. I. (2007) A critical appraisal of the NXY-059 neuroprotection studies for acute stroke: a need for more rigorous testing of neuroprotective agents in animal models of stroke. *Exp. Neurol. 205* (1), 20–25.

(17) Green, A. R., Lanbeck-Vallen, K., Ashwood, T., Lundquist, S., Lindstrom Boo, E., Jonasson, H., and Campbell, M. (2006) Brain penetration of the novel free radical trapping neuroprotectant NXY-059 in rats subjected to permanent focal ischemia. *Brain Res. 1072* (1), 224–226.

(18) Maples, K. R., Ma, F., and Zhang, Y. K. (2001) Comparison of the radical trapping ability of PBN, S-PPBN and NXY-059. *Free Radical Res. 34* (4), 417–426.

(19) Chen, G., Zhang, S., Shi, J., Ai, J., Qi, M., and Hang, C. (2009) Simvastatin reduces secondary brain injury caused by cortical contusion in rats: possible involvement of TLR4/NF-kappaB pathway. *Exp. Neurol. 216* (2), 398–406.

(20) Chen, S. F., Hung, T. H., Chen, C. C., Lin, K. H., Huang, Y. N., Tsai, H. C., and Wang, J. Y. (2007) Lovastatin improves histological and functional outcomes and reduces inflammation after experimental traumatic brain injury. *Life Sci. 81* (4), 288–298.

(21) Wang, H., Lynch, J. R., Song, P., Yang, H. J., Yates, R. B., Mace, B., Warner, D. S., Guyton, J. R., and Laskowitz, D. T. (2007) Simvastatin and atorvastatin improve behavioral outcome, reduce hippocampal degeneration, and improve cerebral blood flow after experimental traumatic brain injury. *Exp. Neurol. 206* (1), 59–69.

(22) Tapia-Perez, J. H., Sanchez-Aguilar, M., Torres-Corzo, J. G., Gordillo-Moscoso, A., Martinez-Perez, P., Madeville, P., de la Cruz-Mendoza, E., and Chalita-Williams, J. (2008) Effect of rosuvastatin on amnesia and disorientation after traumatic brain injury (NCT003229758). *J. Neurotrauma 25* (8), 1011–1017.

(23) Sierra, S., Ramos, M. C., Molina, P., Esteo, C., Vazquez, J. A., and Burgos, J. S. (2011) Statins as neuroprotectants: a comparative in vitro study of lipophilicity, blood-brain-barrier penetration, lowering of brain cholesterol, and decrease of neuron cell death. *J. Alzheimer's Dis. 23* (2), 307–318.

(24) Gonzalez Deniselle, M. C., Lopez Costa, J. J., Gonzalez, S. L., Labombarda, F., Garay, L., Guennoun, R., Schumacher, M., and De Nicola, A. F. (2002) Basis of progesterone protection in spinal cord neurodegeneration. *J. Steroid Biochem. Mol. Biol. 83* (1–5), 199–209.

(25) Jiang, N., Chopp, M., Stein, D., and Feit, H. (1996) Progesterone is neuroprotective after transient middle cerebral artery occlusion in male rats. *Brain Res. 735* (1), 101–107.

(26) Roof, R. L., and Hall, E. D. (2000) Gender differences in acute CNS trauma and stroke: neuroprotective effects of estrogen and progesterone. *J. Neurotrauma 17* (5), 367–388.

(27) Wright, D. W., Kellermann, A. L., Hertzberg, V. S., Clark, P. L., Frankel, M., Goldstein, F. C., Salomone, J. P., Dent, L. L., Harris, O. A., Ander, D. S., Lowery, D. W., Patel, M. M., Denson, D. D., Gordon, A. B., Wald, M. M., Gupta, S., Hoffman, S. W., and Stein, D. G. (2007) ProTECT: a randomized clinical trial of progesterone for acute traumatic brain injury. *Ann. Emerg. Med. 49* (4), 391–402 402 e1–2.

(28) Ishrat, T., Sayeed, I., Atif, F., Hua, F., and Stein, D. G. (2010) Progesterone and allopregnanolone attenuate blood-brain barrier dysfunction following permanent focal ischemia by regulating the

expression of matrix metalloproteinases. *Exp. Neurol. 226* (1), 183−190.

(29) Lee, M., Celenza, G., Boggess, B., Blase, J., Shi, Q., Toth, M., Bernardo, M. M., Wolter, W. R., Suckow, M. A., Hesek, D., Noll, B. C., Fridman, R., Mobashery, S., and Chang, M. (2009) A potent gelatinase inhibitor with anti-tumor-invasive activity and its metabolic disposition. *Chem. Biol. Drug Des. 73* (2), 189−202.

(30) Morrison, J. F., and Walsh, C. T. (1988) The behavior and significance of slow-binding enzyme inhibitors. *Adv. Enzymol. Relat. Areas Mol. Biol. 61*, 201−301.

(31) Copeland, R. A. (2005) *Evaluation of enzyme inhibitors in drug discovery. A guide for medicinal chemists and pharmacologists*, Wiley-Interscience, Hoboken, NJ.